Faceting and stress transfer in the missing-row reconstruction of Ir (110)

Alessio Filippetti[1,2] and Vincenzo Fiorentini[1,3]

(1) Istituto Nazionale per la Fisica della Materia and Dipartimento di Fisica, Università di Cagliari, I-09124 Cagliari, Italy

(2) Department of Physics, University of California, Davis, CA 95616, U.S.A.

(3) Walter Schottky Institut, Technische Universität München, Am Coulombwall, D-85748 Garching bei München, Germany

(February 1, 2008)

We present ab initio total energy and stress calculations for the unreconstructed and (2×1)–missing-row reconstructed Ir (110) and Rh (110) surfaces. We use a model based on ab initio results to show that the (n×1) reconstruction is a faceting transition to a long-wavelength–corrugated (111)-like surface, and find the 3×1 structure to be the most stable for Ir in accordance with experiment. We then use the stress density to analyze the stress increase upon reconstruction, and find it to be due to a changed balance of tensile and compressive contributions in the near-surface region.

Experimental findings[1] clearly support the missing-row reconstruction model for the (110) surfaces of the 5d metals Ir, Pt and Au.[2] The reconstructed surfaces have been observed in a variety of $n \times 1$ structures (presumably not all at equilibrium) whereby n–m out of n atomic rows of first-neighbor atoms, oriented in the $[1\bar{1}0]$ direction, are removed from the $m^{\rm th}$ plane, so that all planes through the $(n{+}1)^{\rm th}$ expose rows to the vacuum. Calculations support the existence of this reconstruction pattern for Au[3,4] and Ir[5] and its absence for Ag[4] and Rh[5]. For Ir, mixed reconstructions patterns with predominantly 3×1 character have been observed,[6] while first-principle calculations[5] confirmed that at least the computationally affordable 2×1 structure is indeed favored over the unreconstructed one. On a different line, surface stress has been investigated both experimentally[7,8] and theoretically[5,9,10] (mostly for Pt, Pd, Rh, and Ir). The behavior and role of stress in the reconstruction remains to be investigated. Also, the stability of n×1 structures has not yet been supported theoretically from first-principle (accurate semiempirical studies exist on Au (110)[3]).

Here we address the existence of the 2×1 reconstruction by means of ab initio calculations. We then set up a model to describe n×1 reconstructions, based on ab initio quantities for the computationally tractable cases. Finally, we analyze the behavior of surface stress using a recently-developed tool, the stress density.[11] In the first-principles local-density-functional calculations we use either fully separable norm-conserving (Ir) or ultrasoft (Rh) pseudopotentials, a plane-wave basis cut off at 40 Ry (Ir) and 30 Ry (Rh), and surface slabs of up to 11 atomic planes, fully relaxing all structures. For further details, see Ref. 5.

Ab initio results – In Table I we report surface energy[12] surface stress[13], and workfunction of the unreconstructed Ir and Rh (110) surfaces, and their changes upon reconstruction. The reconstruction energy $H^{\rm rec}$ is the difference between reconstructed and unreconstructed surface energy, i.e. $H^{\rm rec} < 0$ means favored reconstruction. This is found to be the case for Ir, not for Rh, in agreement with experiment.[1,6] For Ir we find an energy gain of 0.03 eV/atom, close to the ~ 0.05 eV/atom obtained previously[3,4] for Au.

The unreconstructed surfaces are under a large tensile stress (negative in our convention), as already customary from previous work on transition metals.[5,9,10] The stress is appreciably larger for Ir than for Rh due to the influence of relativistic effects[10]), and highly anisotropic: A=$\tau_y^{\rm unrec}/\tau_x^{\rm unrec}$ is 1.89 for Ir and 1.61 for Rh (here $\hat{x} =$ [001] and $\hat{y} = [1\bar{1}0]$). The anisotropy is almost entirely due to relaxations (in the ideal structure we find A=1.17 and 1.11 for Ir and Rh), in agreement with Feibelman's argument[9] that the first-neighbor bonds having a component along the [001] direction can shorten upon relaxation, and relieve a large part of their tensile stress, whereas first-neighbor bonds forming the $[1\bar{1}0]$-oriented atomic rows cannot shrink because of symmetry constraints, and thus conserve the stored tensile stress. Our A-values are similar to Feibelman's[9] for Pt and Pd. Both A and its change upon relaxation are greater for the 5d elements – that is, the larger the surface stress, the larger the portion of stress relieved by the relaxation.

Reconstruction causes a puzzling behavior of the surface stress and workfunction. As a tensile stress is negative by convention, negative $\Delta\tau$'s such as those in Table I indicates an increase in tensile stress. The puzzling result is thus that the surface stress is more tensile on the reconstructed surface than on the unreconstructed one. This feature is surprising, as the surface stress is mostly stored into the bonds of the $[1\bar{1}0]$-oriented rows, and one would expect it to decrease upon removal of one row out of two. In addition, the workfunction increases with reconstruction, suggesting a decrease in surface roughness. This is surprising because reconstruction decreases the surface atomic density and apparently increases the roughness (the corrugation amplitude is doubled). (Although this is not our concern here, we note that stress does not decrease upon the 2×1 transition, which seems to disagree with arguments[8] to the effect that stress is the driving force of this transformation. Stress has been invoked to explain e.g. the mesoscopic patterning of period ~ 1500 Å recently observed[7] on 2×1 Pt (110): that, however, is a further transformation of the 2×1-reconstructed surface.)

The faceting model – The increase in workfunction and surface stress with reconstruction can be explained easily if we view the reconstruction as a microfaceting process into (111)-like facets to vacuum. In previous works,[3,14] faceting had already been suggested as a key feature of the missing-row reconstruction: using our first-principle results, we now set up a model giving quantitative evidence in favor of the faceting hypotesis. We then extend it to arbitrary n. The reconstructed surface, sketched in Figure 1, has (111)-oriented facets (shaded areas) at an angle of $\simeq \pm 35^\circ$ from the (110) plane. The average coordination number and bonding geometry of the facet atoms are the same as on the (111) face, suggesting that the facets may exhibit properties close to those of the (111) surface.

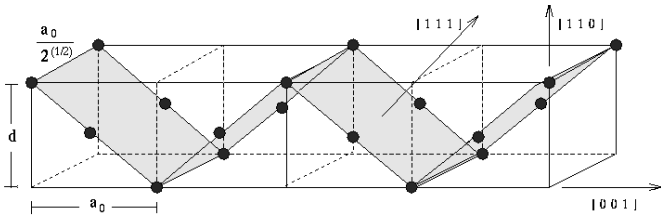

FIG. 1. Faceting model geometry for the missing-row reconstruction: the shaded area is the quasi-(111) reconstructed surface.

We verify such a similarity in a simple but stringent way, comparing directly-calculated first-principles energies and stresses for the reconstructed surface with a model assuming the energy and the stress per unit facet area to be equal to those of the relaxed (111) surface (also calculated ab initio), and integrating these values over the facet area:

$$\sigma^{\rm rec}_{2\times1} = \frac{\sigma_{(111)}}{A^{1\times1}_{(111)}}\,\frac{a_0\,\sqrt{a_0^2+d^2}}{\sqrt{2}}\,. \qquad (1)$$

Here a_0 is the bulk lattice constant, d the first-to-third plane distance (see Figure 1), $\sigma_{(111)}/A^{1\times1}_{(111)}$ the energy per unit area of the relaxed (111) surface. Analogously, for the surface stress we take,

$$\tau^{\rm rec}_{y} = \frac{\tau_{(111)}}{A^{1\times1}_{(111)}}\,\frac{a_0\,\sqrt{a_0^2+d^2}}{\sqrt{2}}\,, \qquad (2)$$

and for $\tau^{\rm rec}_x$ the projection of $\tau^{nr}_{(111)}$ along $\hat{x}$. For the unrelaxed surface, $d = a_0/\sqrt{2}$, and $\sigma^{\rm rec} = 2\,\sigma_{(111)}$. In Table II we compare the ab initio and model-derived values for the relaxed surfaces. The agreement of the two independent evaluations is indeed very good. It is then plausible to identify the 2×1 reconstructed (110) surface with a spatially modulated 'quasi-(111)', quite similar to the true (111) surface. The effect of outward and inward edges appears to nearly compensate each other on average, and the reconstruction can be thought of as a transition from a rough surface (the unreconstructed (110)) to a close-packed, high-coordination surface, i.e. the quasi-(111) surface, perturbed by a relatively long-wavelength corrugation (λ=2a_0). Thus, the increase of workfunction is justified as it actually reflects a transition from a (110)-like to a (111)-like situation (the behavior of the surface stress is discussed later).

The model easily explain the different behavior of Ir and Rh: the energetics of reconstruction is governed by the ratio $R = \sigma_{(110)}/\sigma_{(111)}$. From Equation (1) we have that the missing-row reconstruction occurs if

$$\frac{\sigma_{(110)}}{\sigma^{\rm rec}_{2\times1}} = R\,\frac{A_{(111)}}{\frac{a_0}{\sqrt{2}}\,\sqrt{a_0^2+d^2}} \equiv \frac{R}{R_T} > 1\,, \qquad (3)$$

where $A_{(111)} = \sqrt{3}\,a_0^2/4$. Therefore, the surface reconstructs if R is larger than a reconstruction threshold R_T

$$R_T \;=\; 2\sqrt{\frac{2}{3}}\sqrt{1+\left(\frac{d}{a_0}\right)^2} \;\simeq\; 2\sqrt{1+\frac{2}{3}\left(\frac{\Delta d}{d^{\rm id}}\right)}\,, \qquad (4)$$

where Δd is the change of d from its ideal value $d^{\rm id} = a_0/\sqrt{2}$, and the second equality is valid to first order in $(\Delta d/d)$. R_T is in other words the ratio of the facet area (a function of d) to the (111) area. In Table III we report values of R, R_T, and $\Delta d/d^{\rm id}$ for Ir and Rh. If we disregard relaxations (i.e. put $\Delta d = 0$), then R_T=2, and neither Ir nor Rh should reconstruct. The reduction of d (and hence of the facet area) is the essential ingredient for Ir reconstruction. Rh, on the other hand, has nearly equal R_T, but a much smaller R, i.e. a much smaller surface energy anisotropy. Notice however that Rh is actually just on the verge of reconstruction; according to the model, Rh would also reconstruct if it had the same relaxations as Ir (i.e. if the threshold values for Rh and Ir were the same).

An n-dependent faceting model – Th model just discussed is n-independent. Since 3×1 faceted domains have been preferentially observed in experiment,[6] we need to extend the model to a general $n \times 1$ reconstruction. The vertical and horizontal distances between edges and valleys are now given by $d^{\rm ideal}_n = na_0/2\sqrt{2}$ and $d_{\rm horiz} = na_0/2$. The surface energy (per 1×1 area) generalizes to

$$\sigma^{\rm rec}_{n\times1} = \sigma_{(111)}\,\frac{4}{\sqrt{6}n}\sqrt{n^2+\left(\frac{2d_n}{a_0}\right)^2} \qquad (5)$$

where d_n is the distance between first and (n+1)$^{\rm th}$ layer; the threshold ratio becomes

$$R_T(n) = \frac{4}{\sqrt{6}\,n}\sqrt{n^2+\left(\frac{n-\sum_i^n \rho_i}{\sqrt{2}}\right)^2}\,, \qquad (6)$$

with $\sum_i \rho_i = \delta d_n/d^{\rm ideal}_1$ the sum of relaxations expressed as fractions of the ideal interplanar distance. The reconstruction is favored for

$$I = \frac{\sigma^{\rm rec}_{n\times 1} - \sigma_{(110)}}{\sigma_{(111)}} = R_T(n) - R < 0\,. \qquad (7)$$

Since the ρ_i's are not known for layers far away from the top, we assume hypotetical relaxations extrapolating to zero at the tenth plane below the surface the values calculated[5] for the 2×1 case. $I\sigma_{(111)}$ is displayed as circles in Figure 2: the reconstruction is favored for $n \leq 4$.

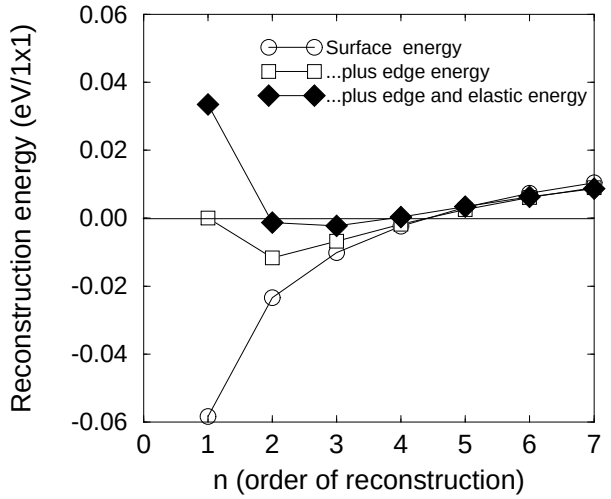

FIG. 2. The (110)–$n \times 1$ reconstruction energy predicted by the faceting model as a function of n (see text).

The monotonic decrease of $I\sigma_{(111)}$ as $n \to 1$ disagrees with two facts: *a)* the 1×1 should be unstable with respect to the 2×1 (although one may simply invoke the inapplicability of the model for n=1); *b)* experiments[1] show that the 3×1 is more stable than the 2×1. To resolve this, one has to account for the contribution of the edges. Adopting a model due to Marchenko[15] and Shchukin *et al.*[16] based on elasticity theory, we add an edge energy and an elastic energy to the reconstruction energy $I\sigma_{(111)}$. The total reconstruction energy is given by

$$\sigma^{\rm rec}_{n\times 1} = I\sigma_{(111)} - \frac{C_1}{n} + \frac{C_2}{n}\ln\frac{n}{2\pi}. \qquad (8)$$

The parameter C_1 is taken to be equal to $I\sigma_{(111)}$, i.e. the energy needed to create on a (111) face the edges and valleys of a (110)–n×1. For C_2, we use[16]

$$C_2 = 8(1-\nu^2)\frac{\tau^2_{(111)}\phi^2}{\pi Y a_0}\,, \qquad (9)$$

with ϕ=0.611 rad $\simeq 35°$ the faceting angle, Y=5.276 Mbar the Young modulus,[17] $\nu = 0.26$ the Poisson ratio,[17] and a_0=7.289 bohr the calculated lattice constant of Ir, $\tau_{(111)} = 1.96$ eV/(1×1) the first-principles calculated surface stress of Ir (111). The successive approximations are depicted in Figure 2. The circles are $I\sigma_{(111)}$; adding the edge energy we obtain (squares) a minimum at n=2, and stable n=3 and n=4; the complete expression (filled diamonds) gives n=2,3 stable with n=3 lowest in energy. The calculated reconstruction energy is not reproduced quantitatively, but its qualitative behavior is now correct.

Explaining the stress increase: application of the stress density – In the light of the faceting model, the rationale for the increase in tensile stress is that reconstruction, while removing rows from the surface, exposes new ones to the vacuum, causing the stress stored in the surface rows atoms to be spatially redistributed, and specifically, transferred towards the substrate. To support this argument directly, we introduced,[11] in analogy to the Chetty-Martin energy density,[18] the stress density, defined as a tensor $\mathcal{T}_{\alpha\beta}(\mathbf{r})$, functional of the charge density, whose integral over the cell equals the macroscopic stress:

$$\int_\Omega d\mathbf{r}\,\mathcal{T}_{\alpha\beta}(\mathbf{r}) = \tau_{\alpha\beta}\,. \qquad (10)$$

The detailed formulation, as well as a discussion of gauge dependence issues, will be given elsewhere.[11] The core idea is that while surface stress only provides information on certain phenomena at surfaces in an integrated fashion, the stress density allows to analyze *locally* its different components. In the present case, we need to consider the planar average $\overline{\mathcal{T}}_{\alpha\beta}(z)$ of the stress density along the [110] direction, and the average of $\overline{\mathcal{T}}_{\alpha\beta}(z)$ over the inter-layer distance (the macroscopic average[19]). In Figure 3, we compare planar and macroscopic average of the stress density of

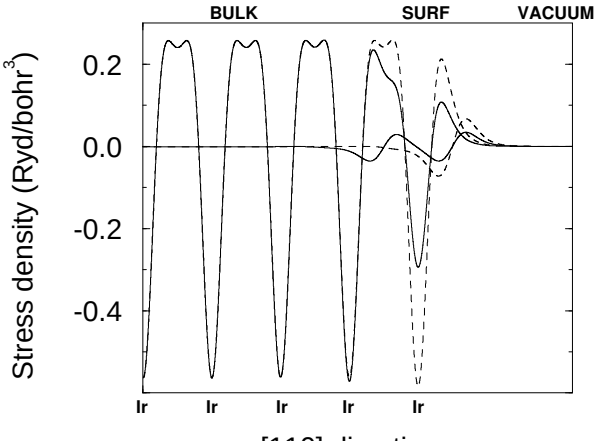

FIG. 3. Planar and macroscopic averages of stress density for the reconstructed (full lines) and unreconstructed (dashed lines) Ir (110) surface.

the unreconstructed (dashed lines) and reconstructed (full lines) surfaces. Both surfaces are considered in their unrelaxed configuration for graphical convenience and, exploiting inversion symmetry, we only display one slab half. Note that the two inequivalent stress components along $\hat{x}$ and $\hat{y}$ are indistinguishable on this scale.

The macroscopic averages vanish into bulk (by the equilibrium condition of vanishing stress) and in the vacuum, and they deviate from zero whenever surface effects arise. Thus, they enable one to establish the effective

boundaries of the surface region as far as stress propagation is concerned. The planar averages show periodic oscillations in the bulk region, and vanish into the vacuum. The negative peaks are tensile contributions arising mostly from electron-ion interactions, and are located at the atomic positions. The positive peaks rising between atomic planes store the compressive stress of essentialy kinetic origin.

The stress transfer upon reconstruction is easily detected moving from left to right in Figure 3: for the unreconstructed surface (dashed line), a non-zero macroscopically-averaged stress density is only visible in the first layer, whereas for the reconstructed one it starts off to non-zero values one layer earlier. The stress is indeed redistributed from the surface to the substrate. Focusing on the planar averages, the negative (tensile) peak in the first layer of the reconstructed surface is reduced with respect to the unreconstructed one. This corresponds to the expected reduction of tensile stress upon removal of the $[1\overline{1}0]$-oriented atomic rows. On the other hand, the positive peak between surface and substrate is also strongly reduced, and it compensates (in fact, overcompensates) the reduction of the tensile component. In other words, row removal reduces the tensile stress in the surface plane, but at the same time it allows electrons to delocalize into the troughs thus created, reducing the compressive kinetic stress. Ho and Bohen[4] arrive at essentially the same conclusion by analyzing the individual contributions to the total energy, and finding a reduction in electron kinetic energy, larger in Au than in Ag.

In summary, we showed that the (110) missing-row reconstruction can be understood as microfaceting of the (110) into a bent, quasi-(111) surface. The reconstruction reduces the effective surface roughness and causes a stress transfer from the surface towards the substrate. The latter effect has been analyzed by means of the stress density. The different behavior between $5d$ and $4d$ elements can be traced back to the greater (110)/(111) surface energy anisotropy, and ultimately to the relativistic character of the heavier elements.[10]

Support from CRS4 Cagliari in the form of computing time on its IBM SP2 is acknowledged. V.F.'s stay at WSI was supported by the Alexander von Humboldt-Stiftung.

[1] For a review see M. A. Van Hove, W. H. Weinberg, and C. -M. Chan, *Low-Energy Electron Diffraction* Springer Series in Surface Science Vol. 6 (Springer, Berlin, 1986).

[2] No reconstruction occurs on the same faces of the corresponding $4d$ elements Rh, Pd, and Ag, except upon alkali metals contamination: R. Schuster, J. V. Barth, G. Ertl, and R. J. Behm, Surf. Sci. Lett. **247**, L229 (1991).

[3] M. Garofalo, F. Ercolessi, and E. Tosatti, Surf. Sci. **188** 321 (1987).

[4] K. M. Ho and K. P. Bohen, Phys. Rev. Lett. **59** 1883 (1987).

[5] A. Filippetti and V. Fiorentini, Surf. Sci. **377**, 112 (1997); A. Filippetti, V. Fiorentini, K. Stokbro, R. Valente, and S. Baroni, in *Materials Theory, Simulations, and Parallel Algorithms*, E. Kaxiras and J. D. Johannopoulos eds., MRS Proc. **408**, 457 (1996).

[6] W. Hetterich and W. Heiland, Surf. Sci. **210**, 129 (1989); H. Bu, M. Shi, F. Masson, and J. W. Rabalais, *ibid.* **230**, L140 (1990).

[7] P.Hanesch and E. Bertel, Phys. Rev. Lett. **79**, 1523 (1997); see also R. Koch, M. Borbonus, O. Haase, and K. H. Rieder, Phys. Rev. Lett. **67**, 3416 (1991).

[8] S. Lehwald *et al.*, Surf. Sci. **192**, 131 (1987).

[9] P. J. Feibelman, Phys. Rev. B **51**, 17867 (1995).

[10] V. Fiorentini, M. Methfessel and M. Scheffler, Phys. Rev. Lett. **71**, 1051 (1993).

[11] A. Filippetti, PhD Thesis, Cagliari University (1997); A. Filippetti and V. Fiorentini, to be published.

[12] V. Fiorentini and M. Methfessel, J. Phys. Cond. Matter **8**, 6525 (1996).

[13] O. H. Nielsen and R. M. Martin, Phys. Rev. Lett. **50**, 697 (1983); Phys. Rev. B **32**, 3780 (1985); *ibid.*, 3792.

[14] G. Binning, H. Rohrer, Ch. Gerber, and E. Weibel, Surf. Sci. **131**, L379 (1983); P. J. Estrup, *Chemistry and Physics of Solid Surfaces* ed. da R. Vanselow e R. Howe, Springer Series of Chemical Physics (Springer-Verlag, Berlin, 1984).

[15] V. I. Marchenko, Sov. Phys. JETP **52**, 605 (1986).

[16] V. A. Shchukin, A. I. Borovkov, N.N. Ledentsov, and D. Bimberg, Phys. Rev. **51**, 10104 (1995).

[17] K. Gschneider, Sol. St. Phys. **16**, 276 (1964).

[18] N. Chetty and R. M. Martin, Phys. Rev. B, **45** 6074 (1992); Phys. Rev. B, **45** 6089 (1992).

[19] A. Baldereschi, S. Baroni, and R. Resta, Phys. Rev. Lett. **61**, 734 (1988); L. Colombo, R. Resta, and S. Baroni, Phys. Rev. B **44**, 5572 (1991).

TABLE I. Surface energy $\sigma^{\rm unrec}$, stresses $\tau_x^{\rm unrec}$ and $\tau_y^{\rm unrec}$, and workfunction $W^{\rm unrec}$ of unreconstructed (110); H^{rec}, ΔW, $\Delta\tau_x$ and $\Delta\tau_y$ are changes in previous quantities upon reconstruction. Results in eV or eV/atom.

	$\sigma^{\rm unrec}$	$H^{\rm rec}$	$W^{\rm unrec}$	ΔW	$\tau_x^{\rm unrec}$	$\Delta\tau_x$	$\tau_y^{\rm unrec}$	$\Delta\tau_y$
Ir	2.59	–0.03	5.42	+0.15	–1.70	–0.44	–3.21	–0.50
Rh	1.89	0.07	5.07	+0.15	–1.25	–0.09	–2.01	–0.13

TABLE II. Reconstruction energies $H^{\rm rec}$ and reconstructed surface stress τ^r (eV/atom) as calculated directly (c) and by the faceting model (m) (see text).

	Ir			Rh		
	$H^{\rm rec}$	$\tau_x^{\rm surf}$	$\tau_y^{\rm surf}$	$H^{\rm rec}$	$\tau_x^{\rm surf}$	$\tau_y^{\rm surf}$
c	–0.03	–2.14	–3.71	0.07	–1.34	–2.14
m	–0.04	–2.20	–3.82	0.03	–1.32	–2.28

TABLE III. $R = \sigma_{[110]}/\sigma_{[111]}$, faceting threshold R_T; relaxation change of first-third layer distance $\Delta d/d^{\rm id}$.

	R	R_T	$\Delta d/d^{\rm id}$
Ir	1.977	1.947	–0.078
Rh	1.948	1.953	–0.069